Solid State Communications 157 (2013) 34–37

Contents lists available at SciVerse ScienceDirect

Solid State Communications

journal homepage: www.elsevier.com/locate/ssc

Control of magnetic anisotropy by external fields in ferromagnetic (Ga,Mn)As

V.F. Sapega [a,b,*], I.V. Kraynov [a], N.I. Sablina [a], G.S. Dimitriev [a], N.S. Averkiev [a], K.H. Ploog [c]

[a] Ioffe Physical Technical Institute, Russian Academy of Sciences, 194021 St. Petersburg, Russia
[b] Spin Optics Laboratory, St. Petersburg State University, 198504 St. Petersburg, Russia
[c] Paul-Drude-Institut für Festkörperelektronik, Hausvogteiplatz 5–7, D-10117 Berlin, Germany

ARTICLE INFO

Article history:
Received 16 November 2012
Received in revised form
25 November 2012
Accepted 9 December 2012
by E.L. Ivchenko
Available online 14 December 2012

Keywords:
A. Ferromagnetic semiconductors
D. Magnetostriction
D. Uniaxial stress

ABSTRACT

We have studied the effect of stress on the magnetic properties of ferromagnetic (Ga,Mn)As diluted magnetic semiconductor. We show that the magnetization of a thin ferromagnetic (Ga,Mn)As layer can be manipulated by uniaxial stress applied in its plane. The effect of stress manifests itself in spin depolarization of holes and stabilizing the easy axis in the direction of the applied stress. The developed theoretical model, assuming stress induced mixing of Mn acceptor-bound hole (or impurity-band bound hole) wave functions, well describes the observed photoluminescence polarization properties in a magnetic field.

1. Introduction

The progress in today's semiconductor electronics originates from the possibility of tailoring the electrical and optical properties. During the last decade intense efforts were made to extend the functionality of semiconductors by making them also magnetic. This possibility was opened up by the discovery of ferromagnetism in the (Ga,Mn)As diluted magnetic semiconductor [1] (DMS). One of the key properties of ferromagnetic (Ga,Mn)As is its magnetic anisotropy, which may be used for the recording of information similar to traditional ferromagnetic materials. So far, a great deal of experimental evidence has been accumulated in manipulating the magnetic properties of (Ga,Mn)As by applying an electric field and varying the doping level [2–8]. Recently, it was demonstrated that the magnetization of a thin ferromagnetic (Ga,Mn)As layer can be modulated by picosecond acoustic pulses [9,10]. In general, the magnetic anisotropy of (Ga,Mn)As films is largely controlled by epitaxial strains [11,12], with tensile and compressive strains inducing in-plane and out-of plane orientation of the magnetic moment, respectively. The strain effects in (Ga,Mn)As have hence been controlled so far by lattice-parameter tailoring during growth [13,14] as well as through post-growth lithographic patterning [15–17]. In this letter we present a direct study of uniaxial stress effects on the magnetic anisotropy of (Ga,Mn)As layers as well as on the spin polarization of ferromagnetism mediating holes. The effect has been studied by means of polarized hot electron photoluminescence (HPL) which is sensitive to the magnetic field as well as to the applied stress. Our study of the HPL polarization demonstrates that in plane stress increases the constant of the uniaxial magnetic anisotropy and leads to a decrease of the hole spin polarization. The latter effect is explained by a stress induced wave function mixing of the ground state of Mn acceptor-bound holes or holes located in the impurity band. The increase of the uniaxial anisotropy energy with stress is explained by an analysis of the potential energy of magnetization in the concurrent presence of magnetic and stress fields.

2. Experimental

The 600 and 800-nm-thick (Ga,Mn)As films for this study were grown at 250 °C by molecular beam epitaxy on semi-insulating GaAs (001) substrates covered with 100-nm GaAs buffer layers. The ferromagnetic (FM) samples studied here have a Mn content of $x=0.043$ (sample A) and $x=0.06$ (sample B). In addition, a Mn-doped 1000-nm-thick GaAs film with $x\sim10^{-5}$ grown at 540 °C was used as reference sample (R). The laser power density focused on the sample was varied in the range from 100 to 200 W cm^{-2}. The photoluminescence (PL) spectra were dispersed by a Jobin–Yvon U-1000 monochromator equipped with a cooled GaAs photomultiplier. Uniaxial stress was applied in the plane of the epilayer along $\langle 110\rangle$ and perpendicular to the external

* Corresponding author at: Ioffe Physical Technical Institute, Russian Academy of Sciences, 194021 St. Petersburg, Russia. Tel.: +7 812 292 7342; fax: +7 812 297 1017.
E-mail address: sapega.dnm@mail.ioffe.ru (V.F. Sapega).

0038-1098/$ - see front matter © 2012 Elsevier Ltd. All rights reserved.
http://dx.doi.org/10.1016/j.ssc.2012.12.004

magnetic field. The HPL circular polarization was measured at sample temperatures of $T=2$ K in the backscattering geometry using a photoelastic modulator (see [18,19] for details). The degree of circular polarization was defined by the common expression $\rho_c=(I_+-I_-)/(I_++I_-)$, where I_+ and I_- are the intensities polarized like the exciting light or opposite to it, respectively.

3. Results and discussion

To study the effect of stress on the magnetic properties of (Ga,Mn)As by means of HPL, whose polarization properties are sensitive to the magnetic and stress fields, was demonstrated in [20]. Fig. 1a shows the HPL spectra of the FM and R samples. The HPL spectrum of the R sample at low temperatures (see spectrum in Fig. 1a for $T=4$ K) is due to the recombination of hot electrons with holes bound to single Mn-acceptors as illustrated schematically in Fig. 1b. It spreads from the point of electron generation in the conduction (c) band (marked as 0LO) on the high-energy side of the spectra to the bottom of the conduction band. Recombination of equilibrium electrons with holes bound to Mn acceptors contribute to the strong band gap PL peak at 1.41 eV. In the FM sample, on the other hand, the hot electrons rather recombine with holes located in the impurity band. Therefore the HPL high-energy cutoff is blueshifted [18]. In contrast to the doped reference sample, the LT grown DMS samples does not demonstrate any band gap PL [19]. Therefore, the measurements of the PL polarization in a magnetic field have been made in the arbitrary spectral point of HPL marked by arrow in Fig. 1a.

The magnetic field dependence of the circular polarization of the HPL obtained from the FM GaMnAs DMS sample is shown in Fig. 1d and from the paramagnetic sample R sample in Fig. 1c, both under unpolarized excitation. In the stress free state, the magnetic field dependence in the FM sample is identical to that observed in Refs. [18,19] i.e. it saturates at $\rho_c\sim0.2$ in $B_s=0.2$ T. The saturating magnetic field in the FM sample is determined as the point where the linear magnetic field dependence of polarization crosses with the observed polarization plateau. When we increase the applied stress, the level of the polarization plateau decreases, while the saturating magnetic field increases. In Fig. 2 we plot the dependence of the saturating magnetic field on the applied stress. In the stress free paramagnetic R sample the polarization curve measured on the band gap PL peak saturates at 0.7 in agreement with theoretical prediction [20]. The PL polarization in the saturating magnetic field decreases with stress increase similar to the FM sample. In Ref. [20] it was shown that the PL as well as the HPL polarization curve related to Mn acceptors in GaAs is very sensitive to stress. To separate the effect of stress on the PL polarization properties (i.e. optical selection rules) and magnetocrystalline ones in the FM sample we start with the analysis of PL selection rules for a single Mn acceptor undergoing magnetic and stress fields.

In contrast to the nonmagnetic acceptors, the ground state of the Mn acceptor in GaAs is strongly modified by exchange interaction between $3d^5$ electrons with total spin $S=5/2$ and valence band holes with $J=3/2$ [21,20]. The Hamiltonian of this interaction can be written as

$$\hat{H}=-A(\hat{\boldsymbol{J}}\hat{\boldsymbol{S}}) \quad (1)$$

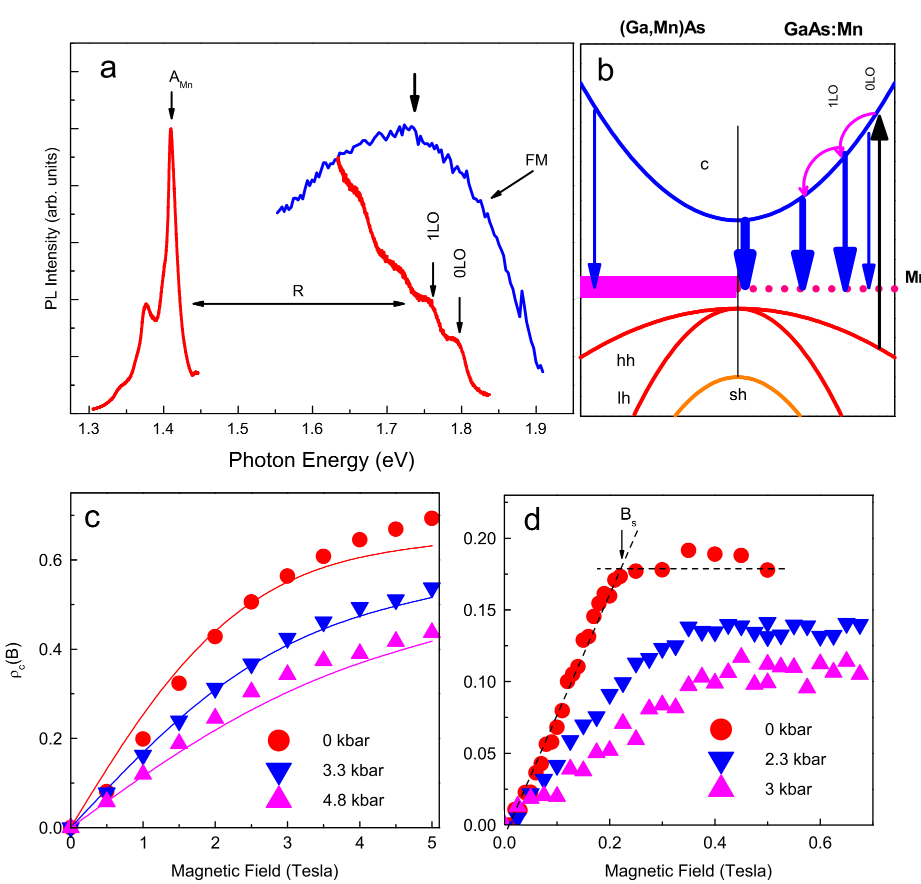

Fig. 1. (Color online) (a) PL and HPL spectra of reference (R) and FM DMS samples (A). Arrow indicates spectral point where polarization curves were measured in FM sample. (b) Scheme of HPL spectroscopy for acceptor bound (right) and impurity-band (left) holes. (c) Polarization curves measured on (R) sample for three different stress values. (d) Polarization curves measured on FM DMS sample (A) for three different stress values.

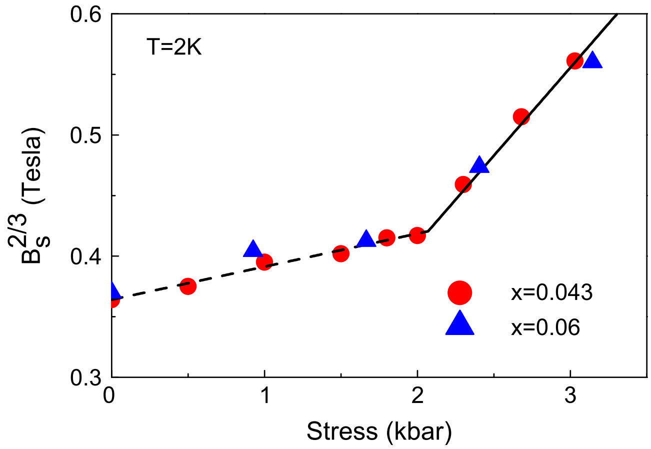

Fig. 2. (Color online) The dependence of $(B_s)^{2/3}$ on applied stress for ferromagnetic samples (A) (circles) and (B) (triangles). Dashed and solid lines are fits by Eqs. (6) and (7) respectively.

where A represents an exchange integral. It was demonstrated in [20–23] that the ground state $F=1(\boldsymbol{F}=\boldsymbol{S}+\boldsymbol{J})$ is obtained via antiferromagnetic exchange interaction of the hole with $3d^5$ electrons of Mn (i.e., $A<0$ in (1)). It is known that the PL circular polarization in a magnetic field in the low temperature limit assumes $+1(-1)$ for nonmagnetic shallow acceptors in GaAs. On the other hand, for Mn acceptors the circular polarization saturates at $-\frac{5}{7}(+\frac{5}{7})$ due to antiferromagnetic exchange. In the ground state the total angular momentum of Mn acceptors ($3d^5+h$ state) equals $F=1$, while the first excited state is shifted by 4.4 meV [23] to higher energies. In the low temperature limit ($T\sim 2$ K) the Mn acceptor properties in a magnetic and stress field can then be described by the following effective Hamiltonian [24]:

$$\hat{H}_{B,P}=\begin{pmatrix} -\frac{q}{2}+\chi & 0 & -i\gamma \\ 0 & q & 0 \\ i\gamma & 0 & -\frac{q}{2}-\chi \end{pmatrix}$$

$$q=\frac{bP}{10(C_{11}-C_{12})},\quad \gamma=\frac{\sqrt{3}dP}{40C_{44}},\quad \chi=\mu_B g_1 B \tag{2}$$

where b, d are deformational potentials of the center, C_{11},C_{12},C_{44} are components of the compliance tensor, and $g_1=\frac{7}{4}g_d+\frac{3}{4}g_h$ (where g_d and g_h are g factors of Mn $3d^5$ electrons and valance band holes respectively) is the g factor of the ground state $F=1$. We assume in Eq. (2) that the uniaxial stress is applied in $\langle 110\rangle$ direction while a magnetic field coincides with the $\langle 001\rangle$ axis. Using the selection rules for optical $\Gamma_6-\Gamma_8$ excitation, the PL circular polarization can be expressed for recombination of equilibrium ($k\sim 0$) electrons with Mn acceptor bound holes as follows:

$$\rho=\frac{5\frac{1-\delta^2}{1+\delta^2}\sinh\left(\frac{\sqrt{(\mu_B g_1 B)^2+\gamma^2}}{kT}\right)}{3e^{-3q/2kT}+7\cosh\left(\frac{\sqrt{(\mu_B g_1 B)^2+\gamma^2}}{kT}\right)},\quad \delta=\frac{\gamma}{\chi+\sqrt{\chi^2+\gamma^2}} \tag{3}$$

Eq. (3) was obtained with the assumption that the equilibrium electrons are not polarized in a magnetic field because $kT>\mu_B g_e B$. Examination of (3) in the high magnetic field limit shows that the circular polarization value ρ_s decreases with increasing stress in the doped sample (see Fig. 1c). This effect is related to wave function mixing of the $Mn^{2+}+h$ state in the stressed sample. Meanwhile the excited states ($F\geq 2$) do not contribute to the ρ_s at $T\sim 2$ K (i.e. $kT\ll A$). The polarization curves presented in Fig. 1c can be well approximated by (3) with deformational potentials b=1.6 eV, d=2.2 eV. We conjecture that the decrease of b and d in comparison to that for shallow acceptors or the top of the valence band is due to strong wave function localization in Mn acceptors [25].

Next we discuss the effect of stress on the HPL polarization curves in FM DMS sample when the Mn content exceeds 10^{20} cm^{-3} and the interaction between Mn acceptors cannot be neglected. In the DMS regime the strong wave function overlap of neighboring Mn acceptors leads to the impurity band formation, thus holes interact with many Mn^{2+} ions. In this case the model of a single Mn acceptor is not valid and we must assume that hole with $J=3/2$ experience an effective mean exchange field induced by the Mn^{2+} ion ensemble. The finding that the polarization curve of the FM sample saturates at much lower field $B_s\sim 0.2$ T (see Fig. 1d) in contrast to the single Mn acceptor ($B_s\sim 6$ T) means that in DMS the strong intrinsic exchange field orients the hole spins in the impurity band. Consequently, the external magnetic field orients the total magnetization of the ensemble, and the hole angular momentum J turns out to be oppositely directed to the intrinsic magnetic fields. To describe the effect of orientation one has to write the density of free energy related to magnetic anisotropy of a sample and the magnetic moment orientation of the system in an applied magnetic and stress field

$$U=M\left\{-\frac{C_1}{2}(m_x^4+m_y^4+m_z^4)+C_2m_z^2-2C_3m_xm_y\right.$$
$$\left.-2\gamma_2\sigma_{xy}m_xm_y-\gamma_1(\sigma_{xx}m_x^2+\sigma_{yy}m_e^2)-m_zB_z\right\}$$
$$\sigma_{xx}=\sigma_{yy}=\sigma_{xy}\equiv\frac{P}{2} \tag{4}$$

where C_iM are energies of anisotropy [26]. In particular, C_1M corresponds to cubic anisotropy, C_2M corresponds to anisotropy, like the "easy axis", while C_3M is related to anisotropy in the plane. γ_i are magnetoelastic coefficients, m_i are direction cosines which are codirectional with the magnetic moment of the sample, M is the magnitude of magnetization, σ_{xy} is the stress tensor, B_z is the external magnetic field, being oriented along the [100] direction. Since C_2M and C_3M are due to internal deformations, we can consider $C_1M\gg C_2M$, C_3M, and neglect any contributions, which are proportional to m_i^4 and $(m_im_j)^2$.

Note, $C_3M>0$ means that the magnetization orients along [110] and $C_3M<0$ the magnetization is parallel to [1$\bar{1}$0]. We can find the equilibrium state of magnetic moment for given values of uniaxial stress and external magnetic field by solving

$$\begin{cases}\frac{\partial U}{\partial\theta}=0\\ \frac{\partial U}{\partial\varphi}=0\end{cases} \tag{5}$$

The solution of the system of (5) uniquely defines the minima of free-energy corresponding to specific orientations of magnetization for given values of σ_{ij} and B_z. In the absence of external magnetic field, the magnetization vector lies in the sample plane. The applied magnetic field continuously drives the magnetization vector out of the plane. When the angle reaches some critical value (θ_s), the magnetization vector abruptly orients along the external magnetic field. Further increase of a magnetic field affects neither the polarization nor the angle θ_s. However, the magnetic field corresponding to the total magnetization does depend on P. The external magnetic field B_s corresponding to the polarization curve saturation can be expressed as

$$B_s=8\sqrt{\frac{(C_1+C_2)^3}{6C_1}}\left(1+\frac{\gamma_1}{2(C_1+C_2)}P\right)^{3/2};\quad P<P_m \tag{6}$$

$$B_s=\sqrt{\frac{(C_1+2C_2+2C_3)^3}{3C_1}}\left(1+\frac{\gamma_1+\gamma_2}{C_1+2C_2+2C_3}P\right)^{3/2};\quad P>P_m \tag{7}$$

Eqs. (6) and (7) clearly show that B_s increases with stress P enhancement. The value of P_m is given by

$$P_m = \frac{(2^{5/3}-1)C_1+2(2^{2/3}-1)C_2-2C_3}{\gamma_2-(2^{2/3}-1)\gamma_1} \tag{8}$$

Fig. 2 shows the dependence of B_s on applied uniaxial stress for ferromagnetic samples A (solid circles) and B (solid triangles). When stress is applied, the magnetization vector orients along the axis of the stress and rotates in external magnetic field in the (P, B) plane. The dependence of $B_s(P)$, presented in Fig. 2, clearly demonstrates the transition from condition Eq. (6) (dashed line) to Eq. (7) (solid line), which accompanies the abrupt change of the curve slope. The kink in the $B_s(P)$ dependence for both A and B samples determines $P_m \approx 2$ kbar. Fits of the data presented in Fig. 2 by means of Eqs. (6) and (7) yield the following constants of magnetic anisotropy $C_1 \approx 510$ Oe cm^{-3}, $C_2 \approx 100$ Oe cm^{-3}, $C_3 = -35$ Oe cm^{-3} and of magnetostriction $\gamma_1 \approx 90$ Oe kbar^{-1}, $\gamma_2 \approx 690$ Oe kbar^{-1}. Comparison of Eqs. (6) and (7) shows that the change of the slope in the $B_s(P)$ curve depends on the C_2/C_1 ratio, which is determined by the contribution of the uniaxial magnetic anisotropy caused by the stress in the growth direction. For the structures studied here we estimate this ratio to be 0.2, which is smaller than that of 0.9 estimated using data from [26]. We conjecture that the lower contribution of the uniaxial magnetic anisotropy in our sample is related to its larger thickness (600−800 nm) in comparison with that (300 nm) studied in [26].

We now analyze the dependence of polarization ρ_s on the applied stress. As in the case of single Mn acceptors, the effect of stress on the HPL polarization can be understood by wave function mixing. In a FM sample the wave functions of holes localized on different potentials can overlap, thus forming the band of delocalized states. In this case, a hole experiences the mean exchange field (Weiss mean field) of all Mn ions. To calculate the HPL circular polarization, we assume that the hole wave function of this narrow band can be calculated using the model of zero radius potential. In this model, the binding energy (E_{loc}) is considered as a parameter, while the symmetry of the hole wave function is considered exactly. The HPL polarization properties are calculated for the recombination of hot electrons (wave vector $k \gg \sqrt{2m_h E_{loc}}/\hbar$) with Γ_8 holes bound to the Mn center.

The explicit form of the spin density matrix of hot electrons in the c band has to include additive terms related to non-zero angular momentum for electrons with non-zero wave vector [20]

$$\hat{\rho}_{ss'} = \delta_{ss'}\left(1+\frac{\alpha}{4}-\frac{3}{4}\alpha\cos^2\theta\right) \tag{9}$$

where α is the parameter describing the anisotropy of momentum distribution, $\delta_{ss'}$ is Kronecker delta. We assume that the exciting laser light propagates along z and the orientation of the electron momentum with respect to z and x-axes is defined by the angles θ, φ. The maximal value of the HPL circular polarization for GaAs ($\alpha=-1$) under unpolarized excitation is then given by the expression

$$\rho = \frac{153-59\nu^2}{177+131\nu^2} \tag{10}$$

Here $\nu = (4b^2C_{44}^2+d^2(C_{11}-C_{12})^2)/(16(C_{11}-C_{12})^2C_{44}d\mu_B g_h)\cdot P/B_{eff}$, where B_{eff} is the intrinsic exchange field. However, the saturation value of HPL observed in the FM sample is much lower than that in the PM sample at the same uniaxial stress. This difference is caused by the larger density of Mn ions which leads to stronger elastic field. This elastic field can be described like random fields, which mixes hole states with different angular momentum [20]. The effect of random fields on the HPL polarization can be taken into account by multiplication of ρ by a factor β. By comparing the polarization calculated (see (10)) for zero external stress ($\rho=0.86$) with the measured $\rho=0.18$ (see Fig. 1d), we estimate a value of $\beta=0.2$. Considering Eq. (10) and the value of the circular polarization in a saturating magnetic field $\rho=0.11$ at P=3 kbar (Fig. 1d), the effective field can then be assumed to be $B_{eff}=15$ T ($\nu=0.6$ at P=3 kbar).

4. Conclusions

We have studied the combined effect of external magnetic and uniaxial stress fields on the magnetic properties of (Ga,Mn)As DMS. In paramagnetic GaAs:Mn effect of magnetic and stress field manifests itself in spin depolarization of acceptor bound holes due to the applied stress. In ferromagnetic (Ga,Mn)As DMS, in addition to the hole spin depolarization, the in-plane uniaxial stress leads to the orientation of the magnetization vector along the applied stress field which stabilizes the easy magnetization axis in the plane of the epilayer. The constants of magnetic anisotropy $C_1 \approx 510$ Oe cm^{-3}, $C_2 \approx 100$ Oe cm^{-3}, $C_3 \approx -35$ Oe cm^{-3}, and of magnetostriction $\gamma \approx 90$ Oe kbar^{-1}, $\gamma_2 \approx 690$ Oe kbar^{-1} have been determined. Our findings demonstrate that a control of the magnetization in (Ga,Mn)As DMS can be realized by appropriate external stress and magnetic fields.

Acknowledgments

We thank M. Moreno for the growth of the samples under investigation. The financial support from the Russian Foundation for Basic Research Grant no. 12-02-00141, Russian Ministry of Education and Science (contract no. 14.740.11.0892, contract no. 11.G34.31.0001 with SPbSPU and leading scientist G.G. Pavlov), RF President Grant NSh-5442.2012.2 is acknowledged.

References

[1] H. Ohno, et al., Appl. Phys. Lett. 69 (1996) 363.
[2] D. Chiba, et al., Nature (London) 455 (2008) 515.
[3] M. Overby, et al., Appl. Phys. Lett. 92 (2008) 192501.
[4] A.W. Rushforth, et al., Phys. Rev. B 78 (2008) 085314.
[5] C. Bihler, et al., Phys. Rev. B 78 (2008) 045203.
[6] M. Glunk, et al., Phys. Rev. B 79 (2009) 195206.
[7] E. De Ranieri, et al., New J. Phys. 10 (2008) 065003.
[8] Sunjae Chung, et al., Solid State Commun. 149 (2009) 1739.
[9] A.V. Scherbakov, et al., Phys. Rev. Lett. 105 (2010) 117204.
[10] M. Bombeck, et al., Phys. Rev. B 85 (2012) 195324.
[11] A. Shen, et al., J. Cryst. Growth 175/176 (1997) 1069.
[12] U. Welp, V.K. Vlasko-Vlasov, X. Liu, J.K. Furdyna, T. Wojtowicz, Phys. Rev. Lett. 90 (2003) 167206.
[13] T. Dietl, H. Ohno, F. Matsukura, Phys. Rev. B 63 (2001) 195205.
[14] M. Abolfath, T. Jungwirth, J. Brum, A.H. MacDonald, Phys. Rev. B 63 (2001) 054418.
[15] J. Wunderlich, A.C. Irvine, J. Zemen, V. Holý, A.W. Rushforth, E. De Ranieri, U. Rana, K. Výborný, Jairo Sinova, C.T. Foxon, R.P. Campion, D.A. Williams, B.L. Gallagher, T. Jungwirth, Phys. Rev. B 76 (2007) 054424.
[16] J. Wenisch, C. Gould, L. Ebel, J. Storz, K. Pappert, M.J. Schmidt, C. Kumpf, G. Schmidt, K. Brunner, L.W. Molenkamp, Phys. Rev. Lett. 99 (2007) 077201.
[17] S. Hümpfner, K. Pappert, J. Wenisch, K. Brunner, C. Gould, G. Schmidt, L.W. Molenkamp, M. Sawicki, T. Dietl, Appl. Phys. Lett. 90 (2007) 102102.
[18] V.F. Sapega, et al., Phys. Rev. Lett. 94 (2005) 137401.
[19] V.F. Sapega, et al., Phys. Rev. B 73 (2006) 235208.
[20] N.S. Averkiev, et al., Fiz. Tverd. Tela (Leningrad) (1988) 765. [Sov. Phys. Solid State 30 (1988) 438].
[21] I.Ya. Karlik, et al., Fiz. Tverd. Tela (Leningrad) 24 (1982) 3550. [Sov. Phys. Solid State 24 (1982) 2022].
[22] J. Schneider, U. Kaufmann, W. Wilkening, M. Baeumler, F. Köhl, Phys. Rev. Lett. 59 (1987) 240.
[23] V.F. Sapega, T. Ruf, M. Cardona, Phys. Status Solidi B 226 (2001) 339.
[24] G.L. Bir, G.E. Pikus, Symmetry and Strain-Induced Effects in Semiconductors, Halsted, Jerusalem, 1974.
[25] M. Linnarsson, E. Janzén, B. Monemar, M. Kleverman, A. Thilderkvist, Phys. Rev. B 55 (1997) 6938.
[26] Xinyu Liu, Jacek K. Furdyna, J. Phys. Condens. Matter 18 (2006) R245.